Applied Acoustics 74 (2013) 356–363

Contents lists available at SciVerse ScienceDirect

Applied Acoustics

journal homepage: www.elsevier.com/locate/apacoust

# Acoustic horns optimization using finite elements and genetic algorithm

Renato Barbieri [a,b], Nilson Barbieri [a,c,*]

[a] Pontifícia Universidade Católica do Paraná – PUCPR, Rua Imaculada Conceição, 1155, CEP 80215-901, Curitiba, Paraná, Brazil
[b] Faculdade de Engenharia de Joinville, Campus Universitário s/n, CEP 89224-100, Joinville, Santa Catarina, Brazil
[c] Universidade Tecnológica Federal do Paraná – UTFPR, Rua Sete de Setembro, 3165, CEP 80230-901, Curitiba, Paraná, Brazil

ARTICLE INFO

*Article history:*
Received 8 August 2011
Received in revised form 18 September 2012
Accepted 25 September 2012
Available online 24 October 2012

*Keywords:*
Acoustic horn
Shape optimization
Finite elements
Genetic algorithm

ABSTRACT

In this work the optimization of shape (geometry) of acoustic horns is analyzed. The finite element method is employed for calculating the sound pressure and optimization methods of zero order (Golden Line Search Method and Genetic Algorithm, GA) are used to obtain the optimal geometry. The shape of the horn is approximated locally using polynomials with $C^1$ continuity with the objective to get a few design variables, to obtain smooth contours at each iteration and to eliminate the regularization of the common mesh in this type of optimization. It was also studied the influence of the size of the domain (environment) in the optimized geometry of the horn. The numerical results show the efficiency of this approach and it was also found (at least from the engineering point of view) that the solution is not unique to the geometry of the horn to single-frequency.



## 1. Introduction

This paper presents the steps and procedures used for the optimization of acoustic horns, as the one shown in Fig. 1. The shape of the waves that propagate in the output of the horn can be cylindrical for problems with planar symmetry and spherical for problems with cylindrical symmetry. Finite Element Method (FEM) was used to calculate the sound pressure, and the shape optimization was performed using two different methods were used: the "Golden Line Search Method" which is employed for the problems with only one design variable, and the Genetic Algorithm method (GA), employed for the other situations.

The modeled domain and the region where the variation in the horn shape is allowed are shown in Fig. 2. In this figure, $\Gamma_{in}$ indicates the inflow boundary (inlet straight tube), $\Gamma_{out}$ denotes the outer domain boundary (free air), which is defined by the radius $R_\Omega$. The horn walls are assumed rigid.

As reported by Bängtsson et al. [1] the problem of analyzing the impedance and radiation properties of acoustic horns has been treated extensively by several authors [2–6]. An excellent review of the mathematical concepts involving the problem and its numerical implementation was carried out by [1]. These authors performed the shape optimization of acoustic horns also employing the Finite Element Method (FEM) and the BFGS quasi-Newton algorithm, which uses the objective-function gradient that is numerically calculated with perturbation. In order to obtain a new geometry and a finite element mesh for each iteration, velocity fields were used (see [7]). In the present work, zeroth-order gradient-free optimization methods were used and the boundary geometry is controlled by Hermite polynomials with $C^1$ continuity. Then, it is shown that there are two very favorable facts when this approach is used: for each new iteration, the horn boundary is smooth and with no reentrance corners, and the number of design variables for obtaining the optimum geometry is greatly reduced.

Aiming to compare the results with the ones obtained by [1], we used the same numerical approach as the one employed by these authors, as summarized below.

## 2. Mathematical formulation and hypotheses

Let denote $\mathbf{x} = (x, y)$ as the coordinates for a point in the $\Omega$ domain and $\mathbf{n}$ the unit normal vector (outward positive direction) on the boundary $\Gamma$. It is assumed the hypotheses that the excitation is only one frequency lower than the inlet tube cut-off frequency, and that the acoustic waves are plane at the entrance of the horn, $\Gamma_{in}$. For these conditions, the expression for the sound pressure perturbation at the entrance of the horn may be written as:

$$P(\mathbf{x}, t) = Ae^{i(\kappa\mathbf{x}\cdot\mathbf{n}+\omega t)} + Be^{i(-\kappa\mathbf{x}\cdot\mathbf{n}+\omega t)} \quad (1)$$

where $\kappa = \Omega/c$ is the typical wave number, $\Omega$ is the wave frequency, $c$ is the speed of sound and $i = \sqrt{-1}$. The $A$ and $B$ terms for this expression correspond to the amplitude of the incident and reflected waves, respectively.

* Corresponding author at: Rua Imaculada Conceição, 1155, CEP 80215-901, Curitiba, Paraná, Brazil. Tel.: +55 41 3271 2211; fax: +55 41 3271 1349.
*E-mail address:* nilson.barbieri@pucpr.br (N. Barbieri).

0003-682X/$ - see front matter © 2012 Elsevier Ltd. All rights reserved.
http://dx.doi.org/10.1016/j.apacoust.2012.09.007

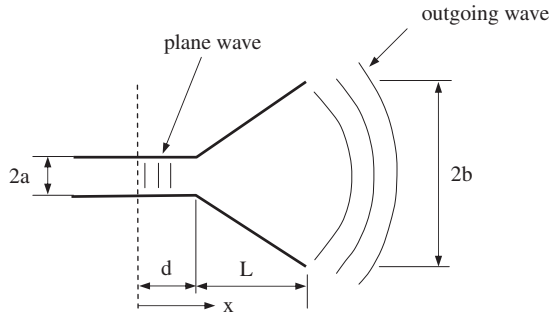


**Fig. 1.** Geometric definitions for the studied acoustic horn (adapted from [1,14]).

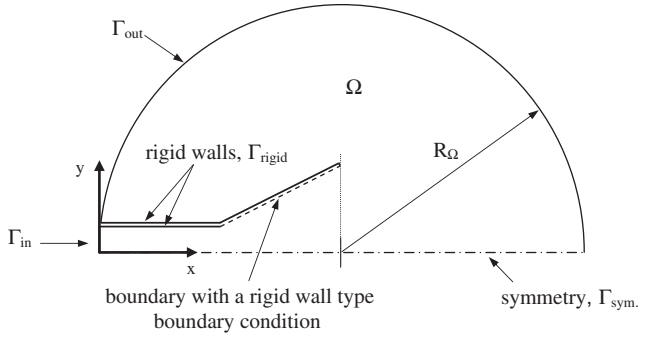


**Fig. 2.** Definition of the design and domain region. (adapted from [1,14]).

Derivation of $P(\mathbf{x}, t)$ in relation to time, $t$, and in relation to the normal **n,** yields:

$$\frac{\partial P(\mathbf{x}, t)}{\partial t} = Ai\omega e^{i(\kappa \mathbf{x}\cdot\mathbf{n}+\omega t)} + Bi\omega e^{i(-\kappa \mathbf{x}\cdot\mathbf{n}+\omega t)} \tag{2}$$

$$\frac{\partial P(\mathbf{x}, t)}{\partial \mathbf{n}} = Ai\kappa e^{i(\kappa \mathbf{x}\cdot\mathbf{n}+\omega t)} - Bi\kappa e^{i(-\kappa \mathbf{x}\cdot\mathbf{n}+\omega t)} \tag{3}$$

Adding these two previous equations and keeping in mind that $\kappa c = \Omega$, we have the expression for the boundary conditions in $\Gamma_{\text{in}}$, i.e:

$$\frac{\partial P(\mathbf{x}, t)}{\partial t} + c\frac{\partial P(\mathbf{x}, t)}{\partial \mathbf{n}} = 2Ai\omega e^{i(\kappa \mathbf{x}\cdot\mathbf{n}+\omega t)} \tag{4}$$

Eq. (4) is satisfied for each wave of the type described in Eq. (1) and can be used to set the amplitude of the incident wave, $A$, in $\Gamma_{\text{in}}$ with no need to know the amplitude of the reflected wave, $B$. Later one, these two amplitudes will be used for defining the *objective function* employed in the shape optimization process of the horn.

On the boundary $\Gamma_{\text{out}}$ Fig. 2, the boundary condition is of the first-order radiation type and it can be found in several sources from the specialized literature, such as [8]. Mathematically, this condition for transient problems may be expressed as following:

$$\frac{\partial P(\mathbf{x}, t)}{\partial t} + c\frac{\partial P(\mathbf{x}, t)}{\partial \mathbf{n}} + \frac{cP(\mathbf{x}, t)}{2R_\Omega} = 0 \tag{5}$$

where $R_\Omega$ represents the outer radius of the domain in analysis, see Fig. 2.

It can be clearly noticed that for $R_\Omega \to \infty$, the third term on the left of Eq. (5) tends to zero. The influence of the $R_\Omega$ value on the horn optimum profile was also one of the factors studied in this paper.

Boundary conditions of Eq. (6) are set for the walls considered rigid and for the symmetry axis:

$$\frac{\partial P(\mathbf{x}, t)}{\partial \mathbf{n}} = 0 \tag{6}$$

Another way to express $P(\mathbf{x}, t)$ defined in Eq. (1) is

$$P(\mathbf{x}, t) = p(\mathbf{x})e^{i\omega t} \tag{7}$$

where $p(\mathbf{x})$ is the complex amplitude of the wave. Substituting this expression into the *Wave Equation*, we obtain the differential equation in the frequency domain known as *Helmholtz Equation* and its respective boundary conditions are obtained from Eqs. (4)–(6). Proceeding this way, the boundary value issue in the frequency domain may be presented in the following way:

$$c^2\Delta p(\mathbf{x}) + \omega^2 p(\mathbf{x}) = 0 \quad \text{in } \Omega \tag{8}$$

$$\left[i\omega + \frac{c}{2R_\Omega}\right]p(\mathbf{x}) + c\frac{\partial p(\mathbf{x})}{\partial \mathbf{n}} = 0 \quad \text{in } \Gamma_{\text{out}} \tag{9}$$

$$i\omega p(\mathrm{x}) + c\frac{\partial p(\mathrm{x})}{\partial \mathbf{n}} = 2i\omega A \quad \text{in } \Gamma_{\text{in}} \tag{10}$$

$$\frac{\partial p(\mathrm{x})}{\partial \mathbf{n}} = 0 \quad \text{in } \Gamma_{\text{rigid}} \cup \Gamma_{\text{sym}} \tag{11}$$

A unified mathematical model for wave propagation in planar or cylindrical symmetry is presented by [14]. The Eqs. (8)–(11) models the wave propagation in planar symmetry that is the condition used in this study. Some results using the cylindrical symmetry condition are presented by [14,15].

### 2.1. The finite-element formulation

The finite-element formulation to obtain the discrete equations for the problem defined in Eqs. (8)–(11) is the Galerkin-FEM. Mathematically we have:

$$\int_\Omega [c^2\Delta p(\mathbf{x}) + \omega^2 p(\mathbf{x})]\phi_j(\mathbf{x})d\Omega = 0 \quad j = 1, 2, \ldots, nf \tag{12}$$

where $\phi_j(\mathbf{x})$ denotes the interpolation functions used in order to approximate $p(\mathbf{x})$. Expanding this expression we have:

$$\int_\Omega [-c^2\nabla p(\mathbf{x})\cdot\nabla\phi_j(\mathbf{x}) + \omega^2 p(\mathbf{x})\phi_j(\mathbf{x})]d\Omega + \int_\Gamma c^2\frac{\partial p(\mathbf{x})}{\partial \mathbf{n}}\tilde{\phi}_j(\mathbf{x})d\Gamma = 0 \tag{13}$$

where $\tilde{\phi}_j(\mathbf{x})$ represents the value $\phi_j(\mathbf{x})$ on the boundary $\Gamma$, i.e., $\tilde{\phi}_j(\mathbf{x}) \cong \lim_{\mathbf{x}\to\Gamma}\phi_j(\mathbf{x})$ .

Dividing all the terms in this equation by $c^2$, we have:

$$\int_\Omega [\nabla p(\mathbf{x})\cdot\nabla\phi_j(\mathbf{x}) - \kappa^2 p(\mathbf{x})\phi_j(\mathbf{x})]d\Omega - \int_\Gamma \frac{\partial p(\mathbf{x})}{\partial n}\tilde{\phi}_j(\mathbf{x})d\Gamma = 0 \tag{14}$$

This expression can also be written in the following matrix form:

$$[K]\{\mathbf{p}\} - \kappa^2[M]\{\mathbf{p}\} - \int_\Gamma \frac{\partial p(\mathbf{x})}{\partial \mathbf{n}}\tilde{\phi}_j(\mathbf{x})d\Gamma = 0 \tag{15}$$

where

$$[K]\{\mathbf{p}\} = \int_\Omega \nabla\phi_i(\mathbf{x})\cdot\nabla\phi_j(\mathbf{x})d\Omega p_n \tag{16}$$

$$[M]\{\mathbf{p}\} = \int_\Omega \phi_i(\mathbf{x})\phi_j(\mathbf{x})]d\Omega p_i \tag{17}$$

In Eqs. (16) and (17) the subscript '*i*' is a integer number and $\phi_i$ $(\mathbf{x})$ $p_i$ denotes the sum $\sum_{i=1}^{nne}\phi_i$ $(\mathbf{x})$ $p_i$ where *nne* is the number of element nodes ($nne = 9$ in this work). This same observation applies to the indexes that appear in Eq. (23). The subscript $i$ of these equations should not be confused with the complex number $i = \sqrt{-1}$ that appears in various other equations text.